SUPPLEMENTARY MATERIAL FOR:

Conformational changes in the P site and mRNA entry channel evoked by AUG recognition in yeast translation preinitiation complexes

Fan Zhang[1], Adesh K. Saini[1.2], Byung-Sik Shin[1], Jagpreet Nanda[3] and Alan G. Hinnebusch[1#]

Fig. S1, Zhang et al.

```
Arabidopsis              MPKNKGKGGKNRKRGKNEADDEKRELIFKEDGQEYAQVLRMLGNGRCEAMCI-DGTKRLC 59
Chlamydomonas            MPKNKGKGGKNRKRGKNENEEEKRELVYKEDGQEYAQVIRMLGNGRLEAQCI-DGKKRLC 59
Saccharomyces            MGKKNTKGGKKGRRGKNDSDGPKRELIYKEEGQEYAQITKMLGNGRVEASCF-DGNKRMA 59
Schizosaccharomyces      MPKNKGKGGKNRRRGKNENENEKRELTYAEEGQMYAQVTKMLGNGRIEAACF-DGVKRLG 59
Homo sapiens             MPKNKGKGGKNRRRGKNENESEKRELVFKEDGQEYAQVIKMLGNGRLEALCF-DGVKRLC 59
Polysphondylium          MPKNKGKGGKNRRRGKNENE-QKRELQFKEDGQEYAQVIKMLGNGRLEAQCF-DGAKRLC 58
Caenorhabditis           MPKNKGKGGKNRRRGKNENDFMKRELDLKEEGQEYGQVSKMLGNGRVQVFCF-DGKQRVC 59
Cryptococcus             MPKNKGKGGKNNRRGKKEDGENKRELIFKEDGQEYAQVVKMLGNGRLEAKCQ-DGESRLA 59
Paramecium               MPKNKGRGGKNYRRGKNENL-TKRQLETKEDGQDYAQVIKLLGNGRLICVCLGDSKQRLG 59
                         * *:: :***: :***::    **:*   *:** *.*: ::*****    *  *. .*:
                                                  --------
                         ---------NTT-------------N-strand-----------OB-fold---------

Arabidopsis              HIRGKMHKKVWIAAGDIVLVGLRDYQDDKADVILKYMSDEARLLKAYGELPENTRLNEGI 119
Chlamydomonas            NIRGKMRKKVWVAQGDIVLVGLRDYQDEKADVIMKYTADEARVLKQYGELPEHIRINDTD 119
Saccharomyces            HIRGKLRKKVWMGQGDIILVSLRDFQDDQCDVVHKYNLDEARTLKNQGELPENAKINETD 119
Schizosaccharomyces      HIRGKLRKKVWINQGDIILLSLREFQDEKGDVILKYTADEARTLKNQGELPETAKINETD 119
Homo sapiens             HIRGKLRKKVWINTSDIILVGLRDYQDNKADVILKYNADEARSLKAYGELPEHAKINETD 119
Polysphondylium          HISGRLRKKEWINSGDIILLQLRDYQDDKADVVLRYTIDEARSLKTLGELPETAKINEAD 118
Caenorhabditis           HIRGKLRKKVWINVGDIILVGLRDYQDDKGDVILKYTPDEARRLKNEGLIPENAKLNEND 119
Cryptococcus             QIRGQMRKKVWIVVGDIILLSLRDFQDDRADVIHRYTPDEARNLKTYGELKDFQLVENQE 119
Paramecium               HIRGKMRRKVWIQNGDIVLVALREFQDEKCDVVYKYFPEEIKQLKNLKEIPENLEEGGGD 119
                         :* *::::* *:  .**:*: **::**:: **: :*  :* : **    : :
                                                               --helix--   ----     -
                         ----------OB-fold---------------------         --- 3_10 -----
                                                                         L      Cstrd

Arabidopsis              VGD-------------------------------LEDDDDNNDDDYVEFEDE-------- 140
Chlamydomonas            V---------------------------------IFEGEDKENQEYFDFD---------- 136
Saccharomyces            NFG--------------------------------FESDEDVNFEFGNADEDDEEGEDEE 147
Schizosaccharomyces      TFG--------------------------------AEGEDDLDFEF-------------- 133
Homo sapiens             TFG--------------------------------PGDDDEIQFDDIGDDDE-------- 139
Polysphondylium          TFD--------------------------------EMDG-EIPFEFVADND--------- 136
Caenorhabditis           EQDEGEVEFLDHVGDEGEAGEAKSDSDSSDSDSEKSDEEAGSDKEEESDDDSEEESDEDS 179
Cryptococcus             AGG---------------------------------EEDEEGGIEFEEA----------- 135
Paramecium               NIG-------------------------DNVVFVNKEESSSSDSDISDSDSD-------- 146
                                                                     :
                         -----------------------------CTT----------------------------

Arabidopsis              -DIDRV------------------------------------- 145
Chlamydomonas            -DIAEI------------------------------------- 141
Saccharomyces            LDIDDI------------------------------------- 153
Schizosaccharomyces      -DVDAI------------------------------------- 138
Homo sapiens             -DIDDI------------------------------------- 144
Polysphondylium          -DIVIISSTLHLDIHIHASLINP-------------------- 158
Caenorhabditis           DDSDNIREEDLAAGRGFKEDTRRGGNRGGKNKYGKRR------ 216
Cryptococcus             -DIDDI------------------------------------- 140
Paramecium               -DSSDSEPKQPQKQQPQKPQPQKAQAPAKDNKEKITKKDIDDI 188
                          *
                         -------------------CTT---------------------
```

Figure S1. Alignment of eIF1A sequences from diverse eukaryotes. Structural domains are indicated below the alignments, with helix, L, 3_{10} and Cstrd indicating the helical, loop, 3_{10}-helix, and structured C-strand domains, respectively, in addition to the NTT, OB-fold, and CTT domains, based on the solution structure of human eIF1A (33). Residues substituted with cysteines are shown in the Saccharomyces sequence in red boldface.

Fig. S2, Zhang et al.

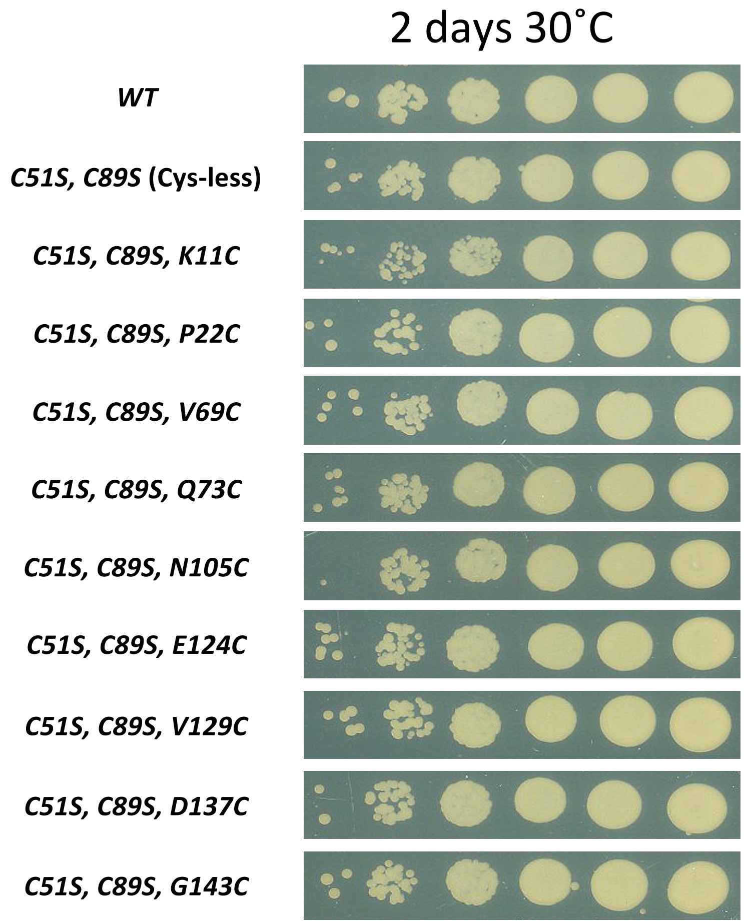

Figure S2. Introduction of novel cysteines has little or no effect on the ability of eIF1A variants to substitute functionally for WT eIF1A in vivo. Growth rates of derivatives of *tif11Δ* strain H3582 (*MATa ura3-52 trp1Δ63 leu2-3 leu2-112 his4-301(ACG) tif11Δ p3392 [TIF11, URA3]*) harboring the indicated WT or mutant *TIF11* alleles as the only *TIF11* allele on single-copy *LEU2* plasmids were determined by spotting serial 10-fold dilutions on YPD medium and incubated for 2 d at 30°C.

Fig. S3, Zhang et al.

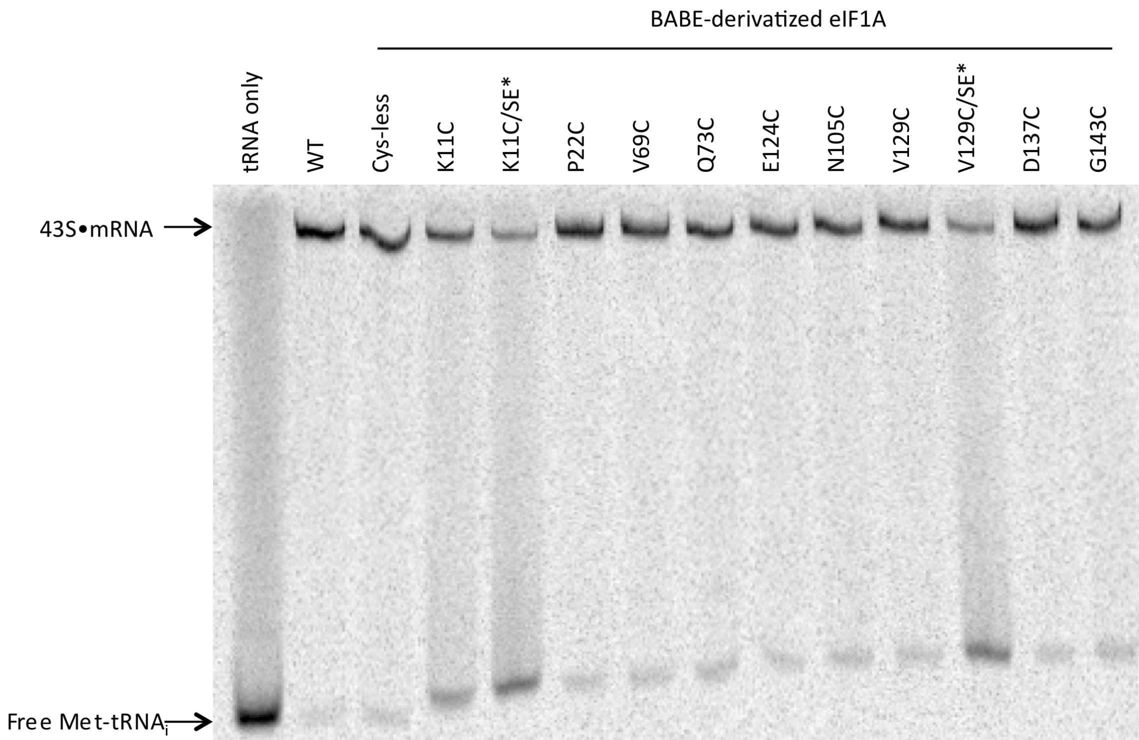

Figure S3. All single-Cys derivatives of eIF1A support efficient assembly of 43S•mRNA PICs. Phosphorimage of a native gel showing 43S•mRNA(AUG) complexes assembled using purified 40S ribosomal subunits, eIF1, pre-formed TC (containing purified eIF2, [^{35}S]-Met-tRNA$_i$, and GDPNP) and the indicated BABE-derivatized eIF1A variants. Reactions were conducted as described in Materials and Methods and loaded onto a running native gel. Lane 1 contains [^{35}S]-Met-tRNA$_i$ only. Free TC dissociates rapidly on entering the gel (36). The apparent diminished migration of free [^{35}S]-Met-tRNA$_i$ from left to right reflects the fact that samples were loaded on the gel at different times.

Fig. S4, Zhang et al.

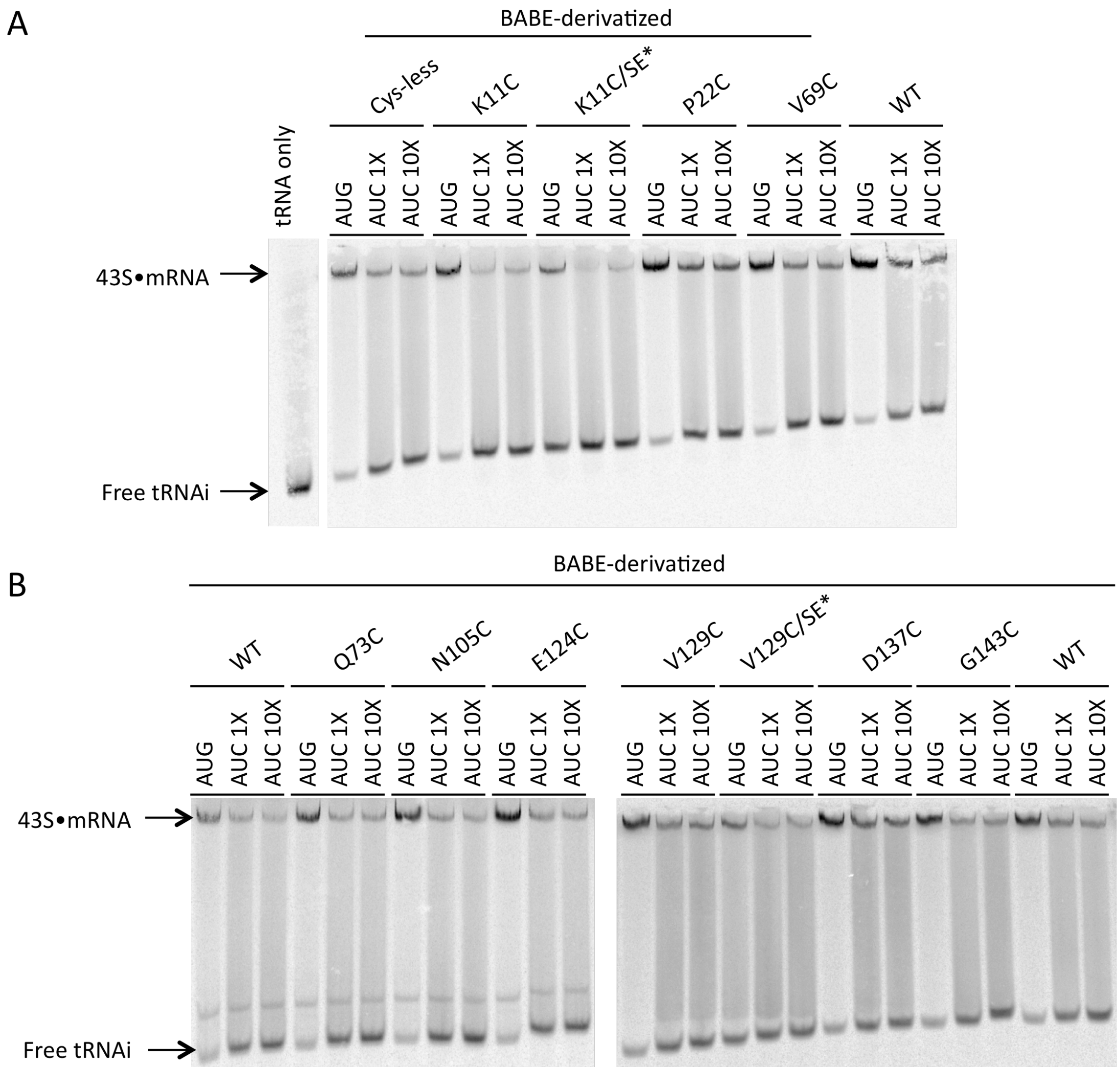

Figure S4. **Increasing the concentration of mRNA(AUC) by an order of magnitude does not increase the end-point of 43S·mRNA PIC assembly. (A-B)** Same as in Fig. S3 except that the indicated reactions contained mRNA(AUC) at the same (1X) or 10-fold higher (10X) concentration of that used for mRNA(AUG). The diminished yields achieved with both concentrations of mRNA(AUC) versus mRNA(AUG) reflects the fact that the open/P_{OUT} conformation of the PIC formed with mRNA(AUC) is less stable than the closed/P_{IN} conformation produced with mRNA(AUG) and dissociates during electrophoresis, giving rise to a smear of [^{35}S]-Met-tRNA$_i$ signal throughout the lane (21,28).

Fig. S5, Zhang et al.

A

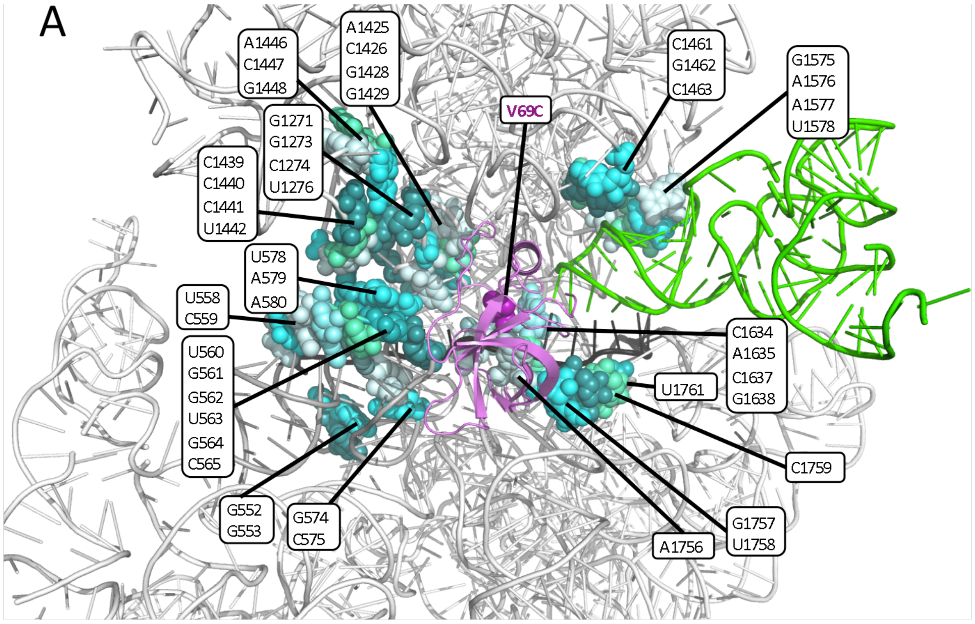

B

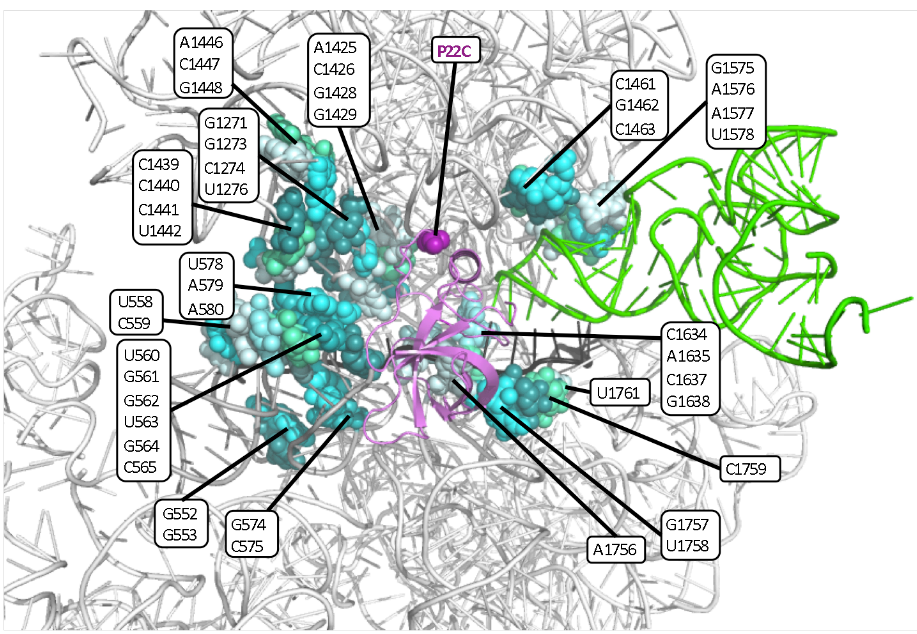

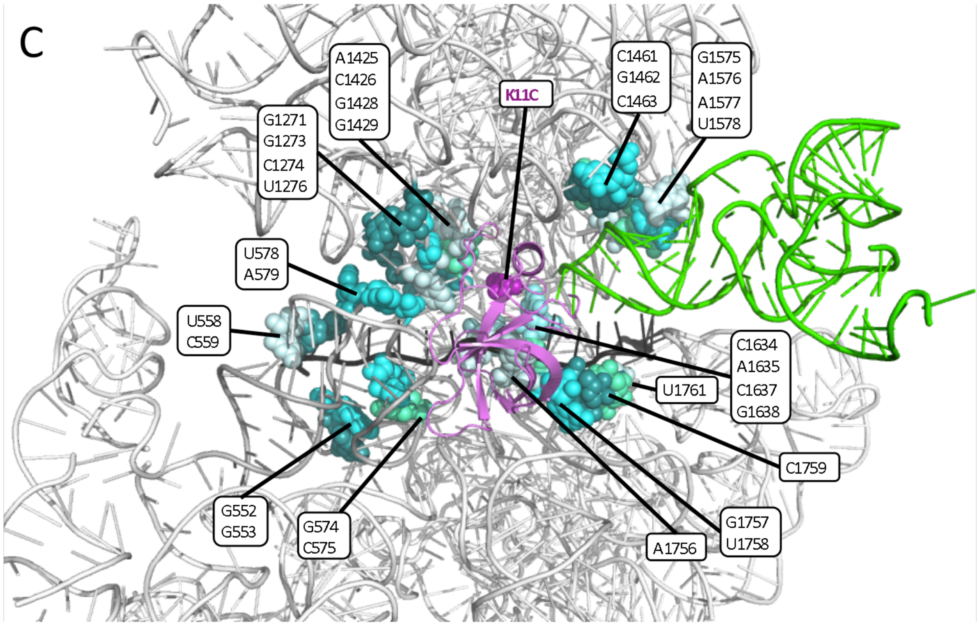

Figure S5. Summary of 18S rRNA residues cleaved by single-Cys variants. (A-C) 18S rRNA residues cleaved by the eIF1A single-Cys variants (labeled with magenta lettering) are depicted as light blue or light green spheres in the yp48S PIC (Hussein et al. 2014), as described in Fig. 2. The locations in eIF1A of the single-Cys residues are depicted with magenta spheres.

Fig. S6, Zhang et al.

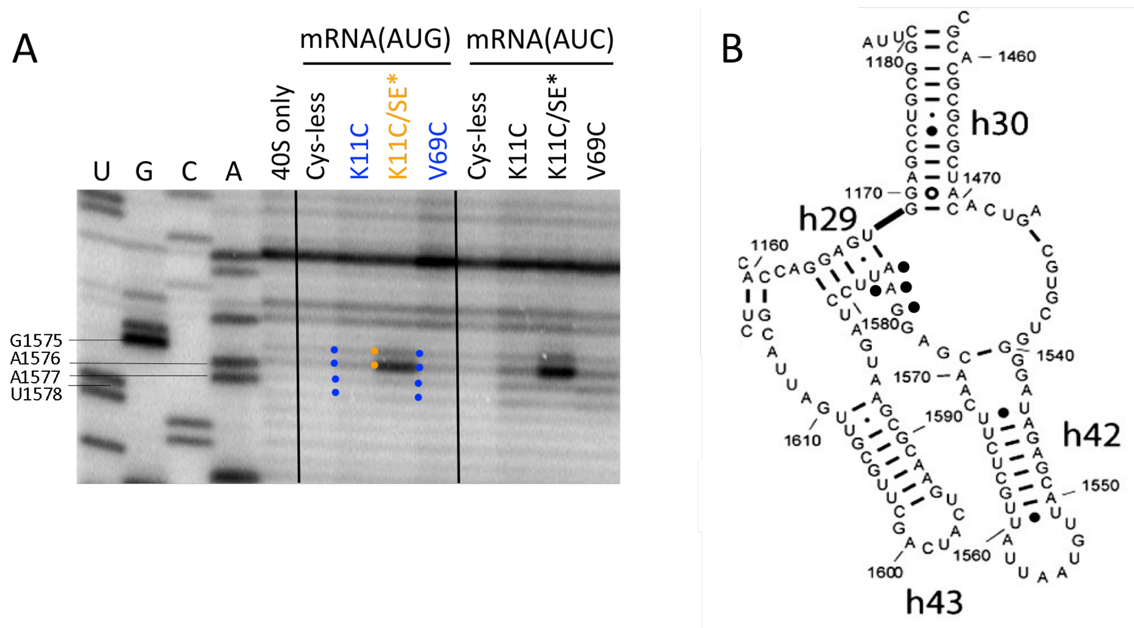

Figure S6. Directed hydroxyl radical cleavage of P-site residues within or proximal to h29 by eIF1A variants K11C and V69C is modulated by start codon recognition in reconstituted PICs. (A-B). Sites of cleavage of 18S rRNA by eIF1A single-Cys variants in PICs assembled with no mRNA, mRNA(AUG) or mRNA(AUC) mapped by primer extension inhibition, as described in Fig. 3.

Fig. S7, Zhang et al.

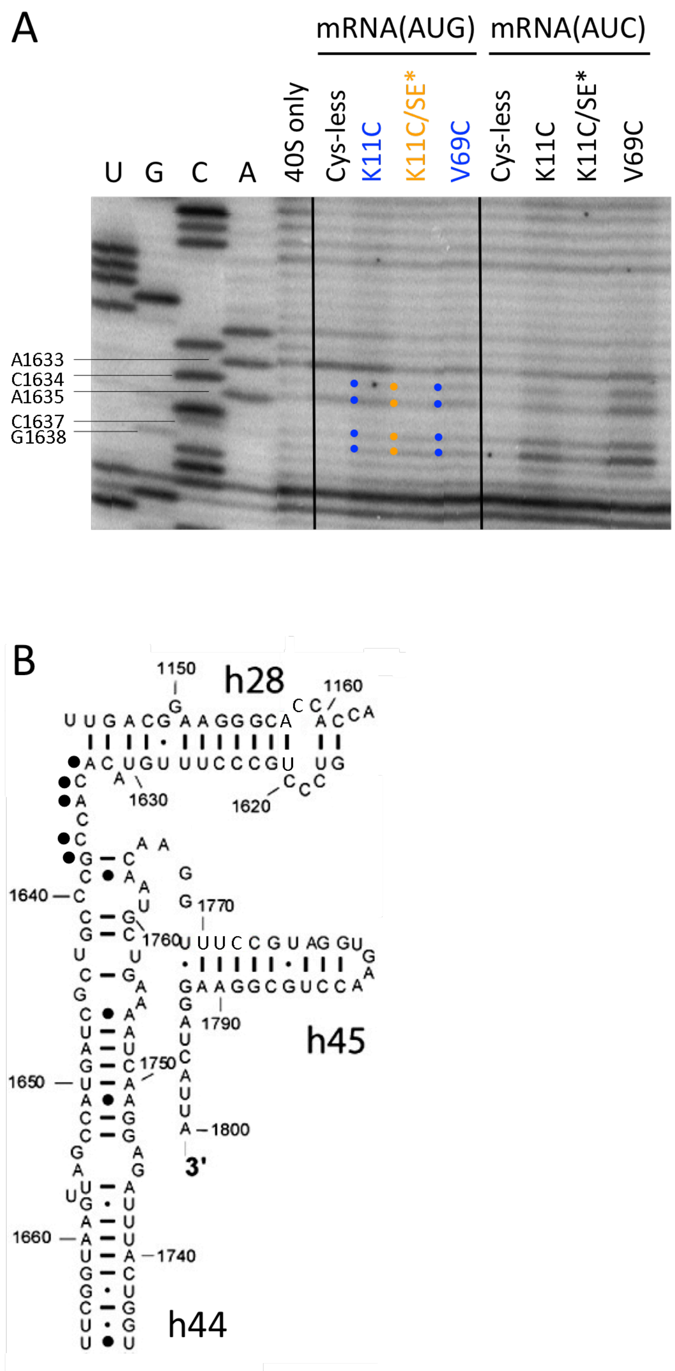

Figure S7. Directed hydroxyl radical cleavage of P-site and A-site residues between h44 and 28 by eIF1A variants K11C, and V69C is modulated by start codon recognition. (A-B). Sites of cleavage of 18S rRNA by eIF1A single-Cys variants in PICs assembled with no mRNA, mRNA(AUG) or mRNA(AUC) mapped by primer extension inhibition, as described in Fig. 3.

Fig. S8, Zhang et al.

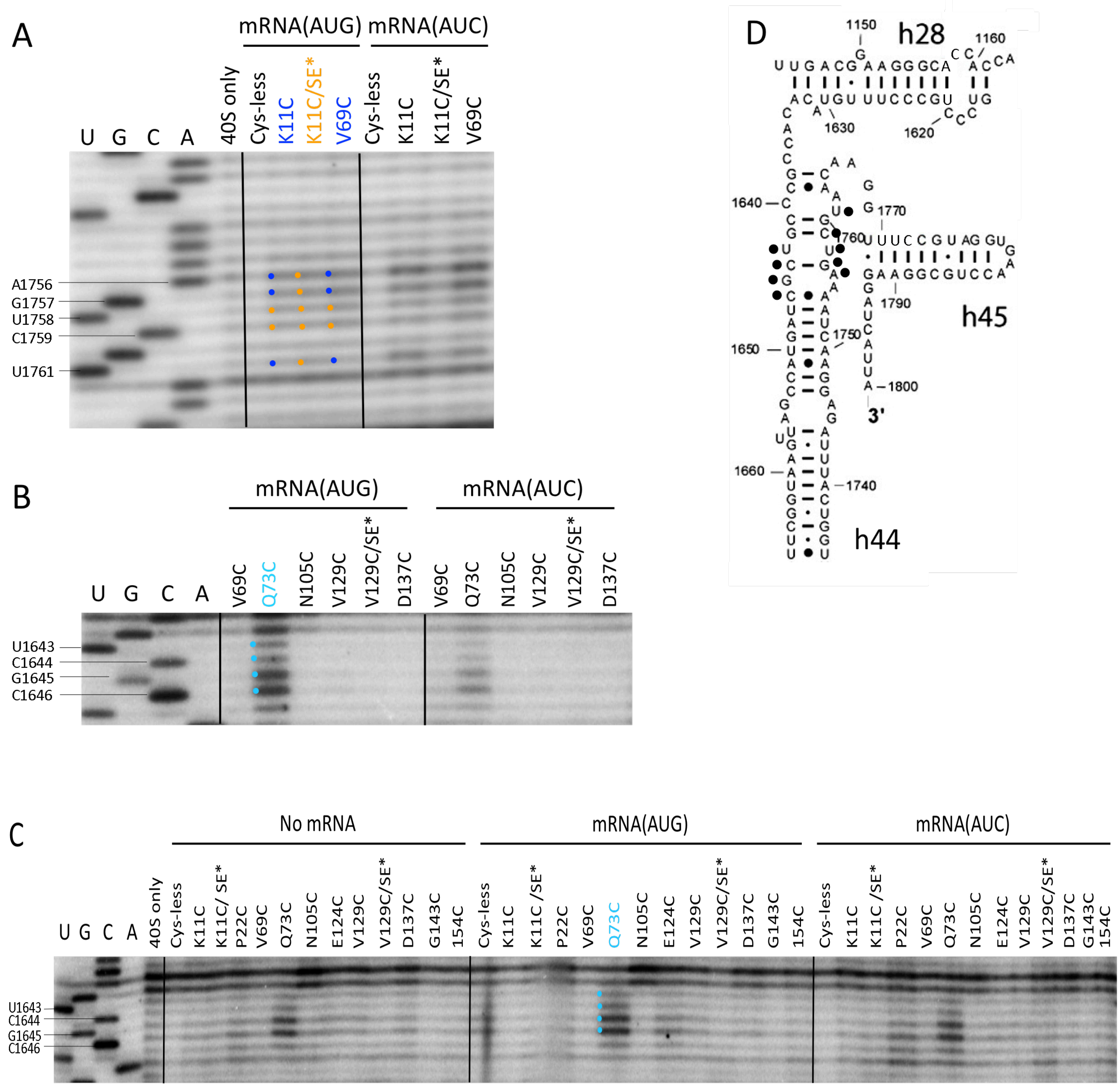

Figure S8. Directed hydroxyl radical cleavage of P-site and A-site residues in h44 by eIF1A variants K11C, P22C, V69C, and Q73C is modulated by start codon recognition. (A-D). Sites of cleavage of 18S rRNA by eIF1A single-Cys variants in PICs assembled with no mRNA, mRNA(AUG) or mRNA(AUC) mapped by primer extension inhibition, as described in Fig. 3.

Fig. S9, Zhang et al.

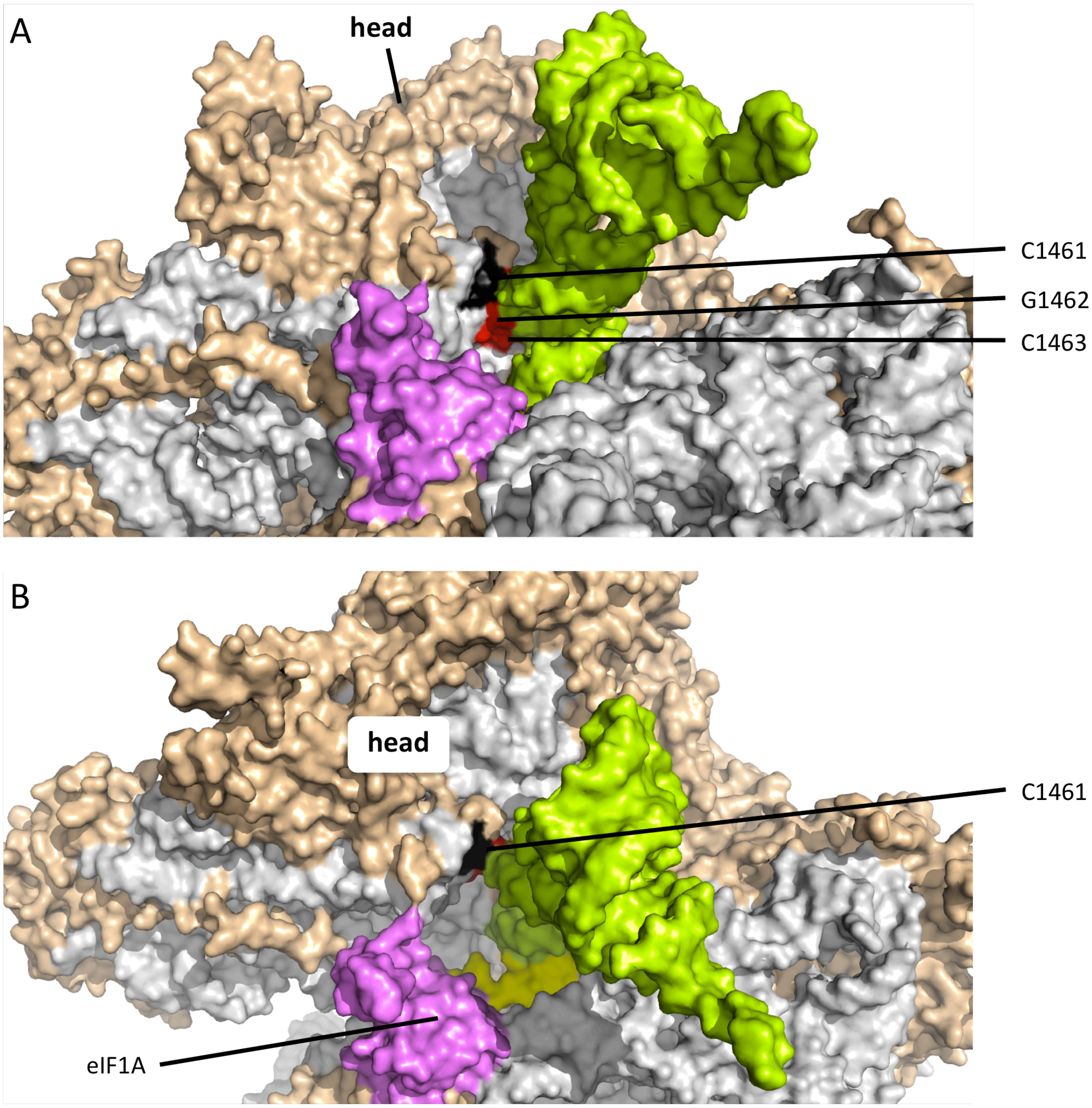

Figure S9. Differential surface exposure of h30 residues C1461, G1462 and C1463. (A-B) PyMOL model of the mp48S PIC (Lomakin & Steitz, 2013), depicted in surface representation with rRNA residues, tRNA$_i$, and eIF1A colored as in Fig. 4 and with mRNA in yellow and ribosomal proteins in wheat). **(A)** Illustrates roughly equal exposure of h30 residues C1461 (black), G1462 (dark orange) and C1463 (deep red) from the vantage point of eIF1A (magenta). **(B)** Illustrates exposure of primarily C1461 (black) from the vantage point of the 40S subunit head.

Fig. S10, Zhang et al.

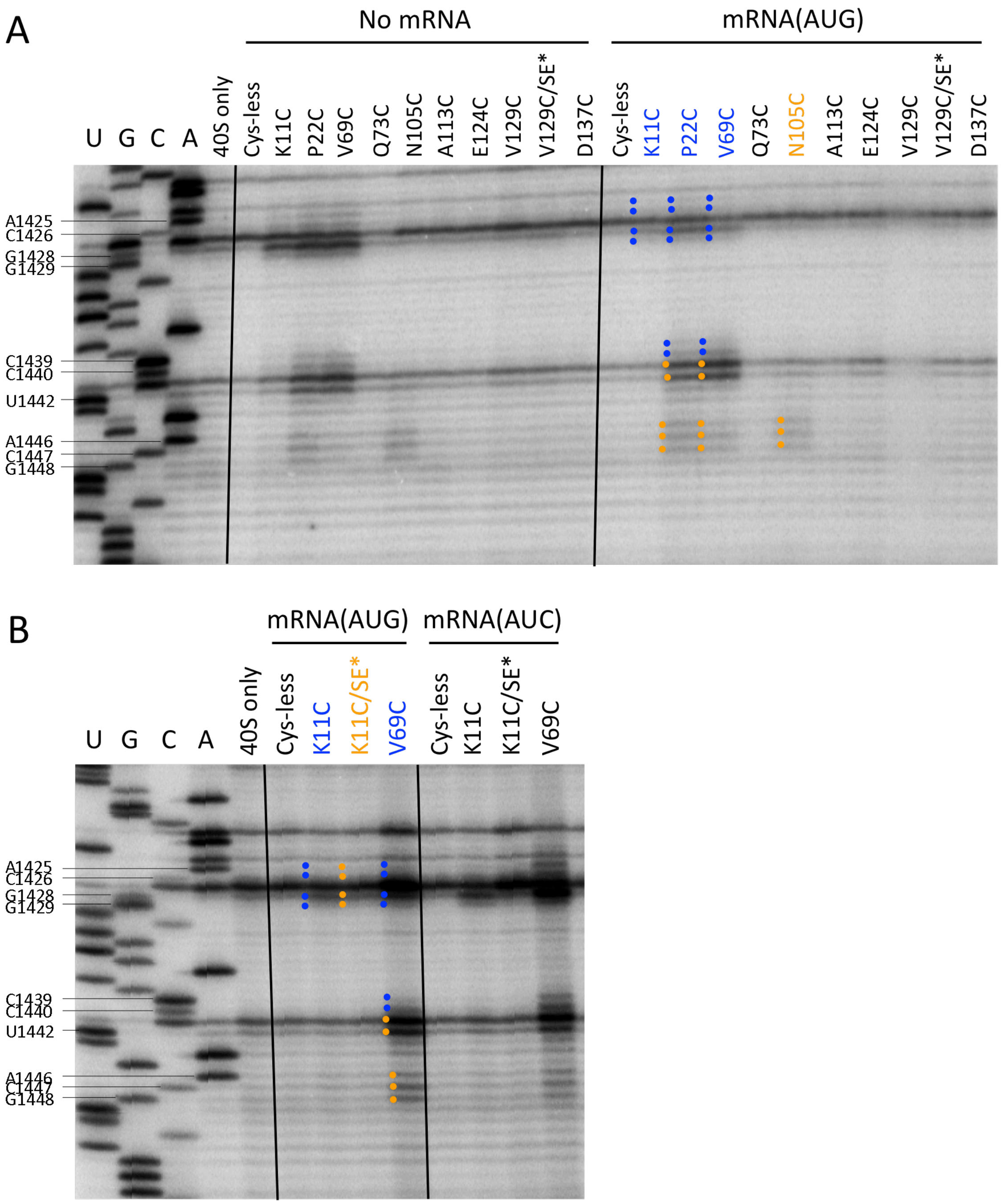

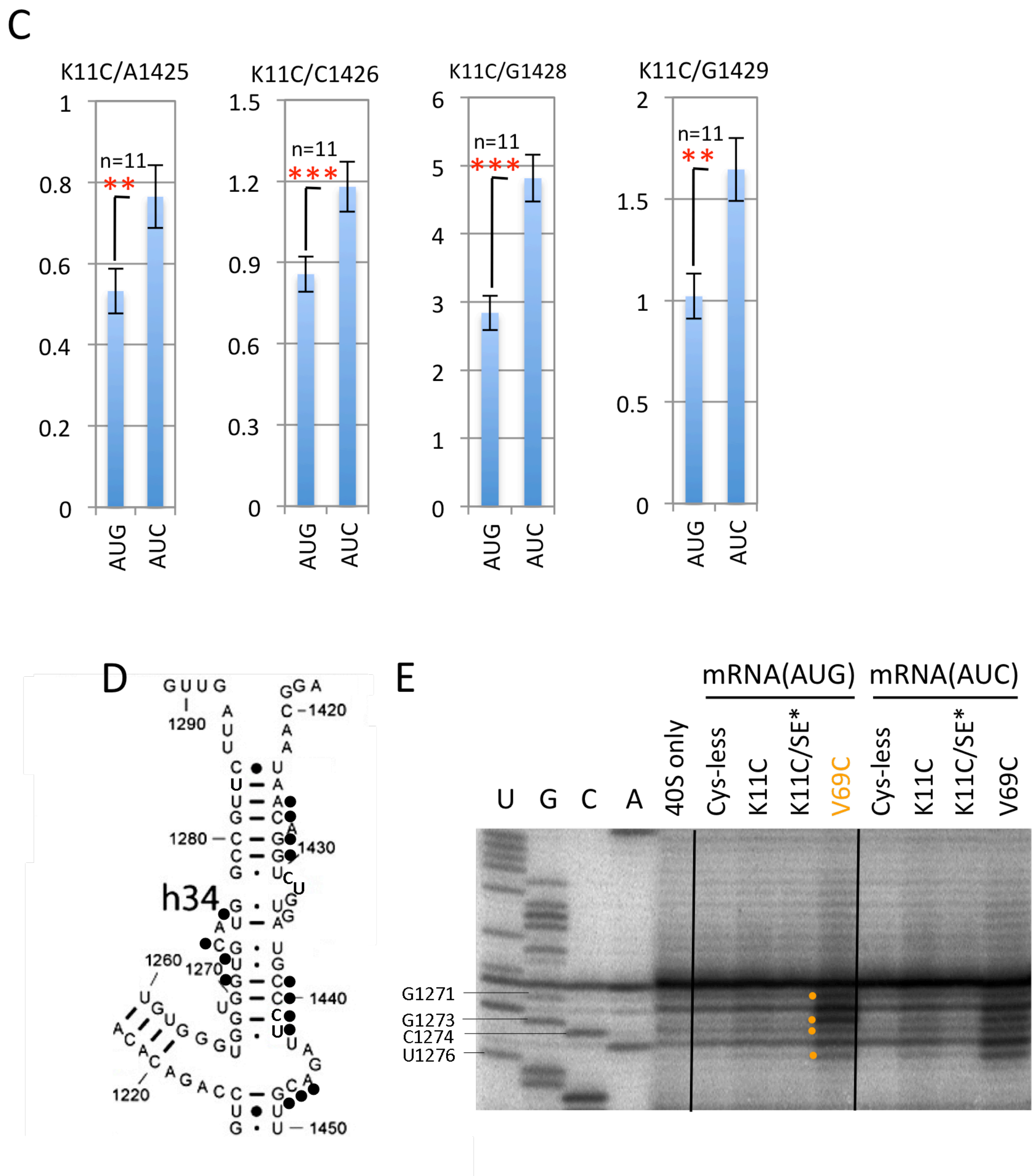

Figure S10. Directed hydroxyl radical cleavage of h34 residues in the upper entry channel or latch region by eIF1A variants K11C, P22C, and V69C is modulated by start codon recognition. (A-C). Sites of cleavage of 18S rRNA by eIF1A single-Cys variants in PICs assembled with no mRNA, mRNA(AUG) or mRNA(AUC) mapped by primer extension inhibition, as described in Fig. 3. **(D)** Cleavage of the indicated residues by the K11C derivative was quantified as described in Fig. 3D.

Fig. S11, Zhang et al.

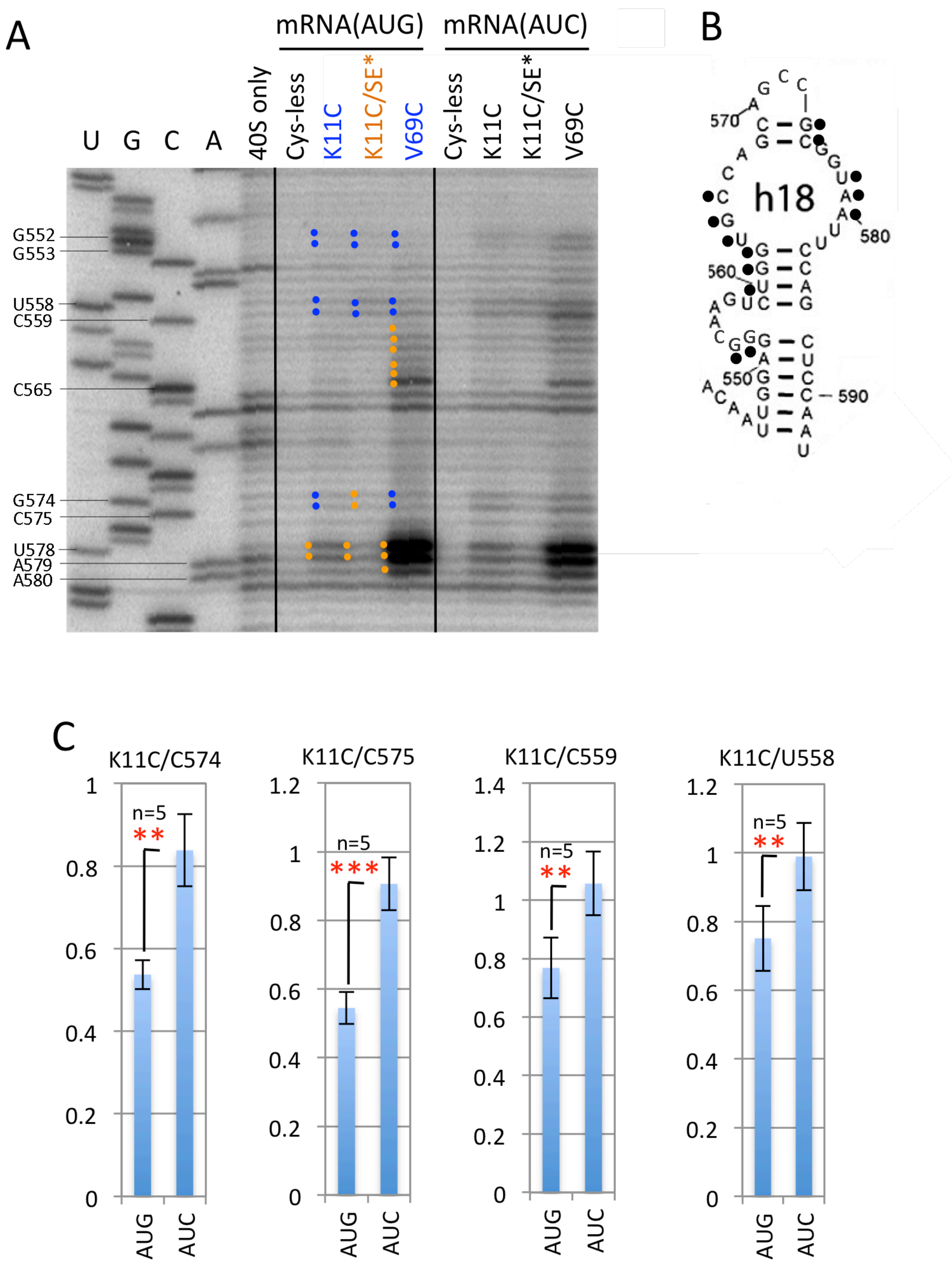

Figure S11. Directed hydroxyl radical cleavage of h18 residues in the lower entry channel or latch region by eIF1A variants K11C, K11C/SE* and V69C is modulated by start codon recognition. (A-B). Sites of cleavage of 18S rRNA by eIF1A single-Cys variants in PICs assembled with mRNA(AUG) or mRNA(AUC) mapped by primer extension inhibition, as described in Fig. 3. **(C)** Cleavage of the indicated residues by the K11C derivative was quantified as described in Fig. 3D.

Fig. S12, Zhang et al.

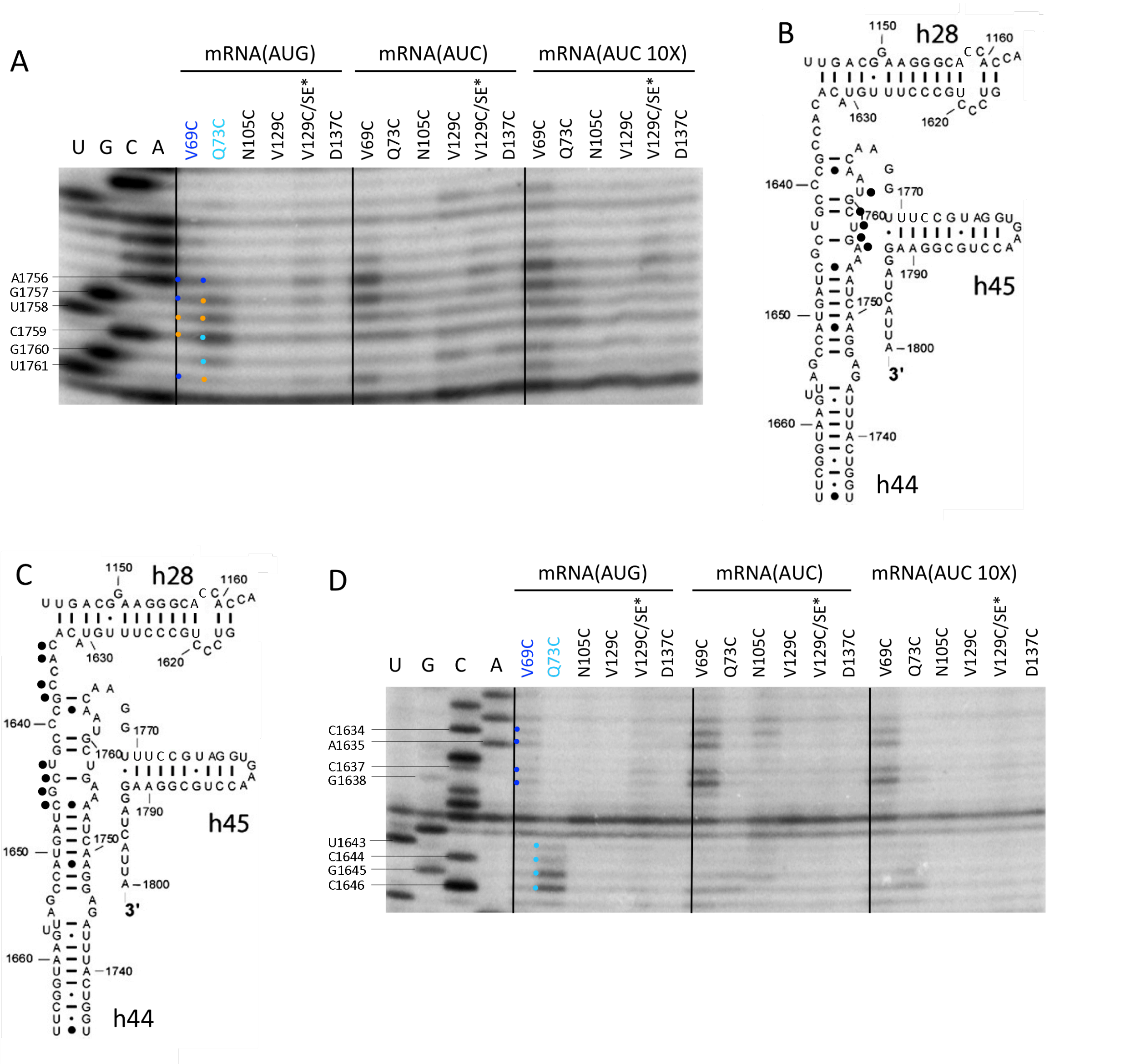

Figure S12. Increasing the concentration of mRNA(AUC) by an order of magnitude does not appreciably alter patterns of AUC>AUG cleavage or response to the SE* substitutions in h44 (A-B and C-D) and between h44 and h28 (C-D). Experiments were conducted and results presented exactly as described for Figs. 3, and 5-9 except that PICs assembled with a 10-fold higher concentration of mRNA(AUC) were analyzed in parallel with PICs assembled at the standard concentrations of mRNA(AUC) and mRNA(AUG). **(D)** Cleavage of the indicated residues by the K11C derivative was quantified as described in Fig. 3D.

Fig. S13, Zhang et al.

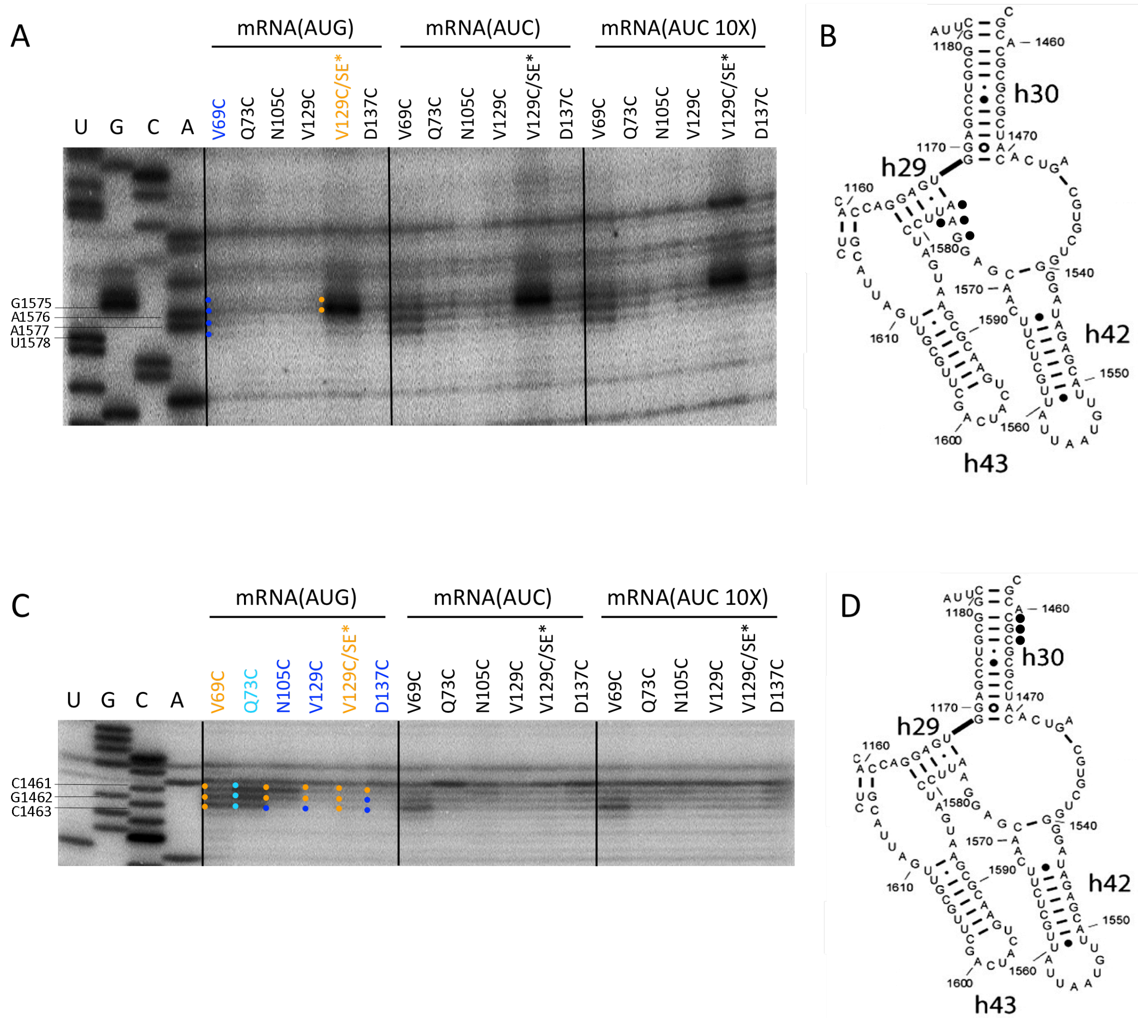

Figure S13. Increasing the concentration of mRNA(AUC) by an order of magnitude does not appreciably alter patterns of AUC>AUG cleavage or response to the SE* substitutions in h29 and between h29 and h42 (A-B); and in h30 (C-D). Experiments were conducted and results presented exactly as described for Figs. S11.

Fig. S14, Zhang et al.

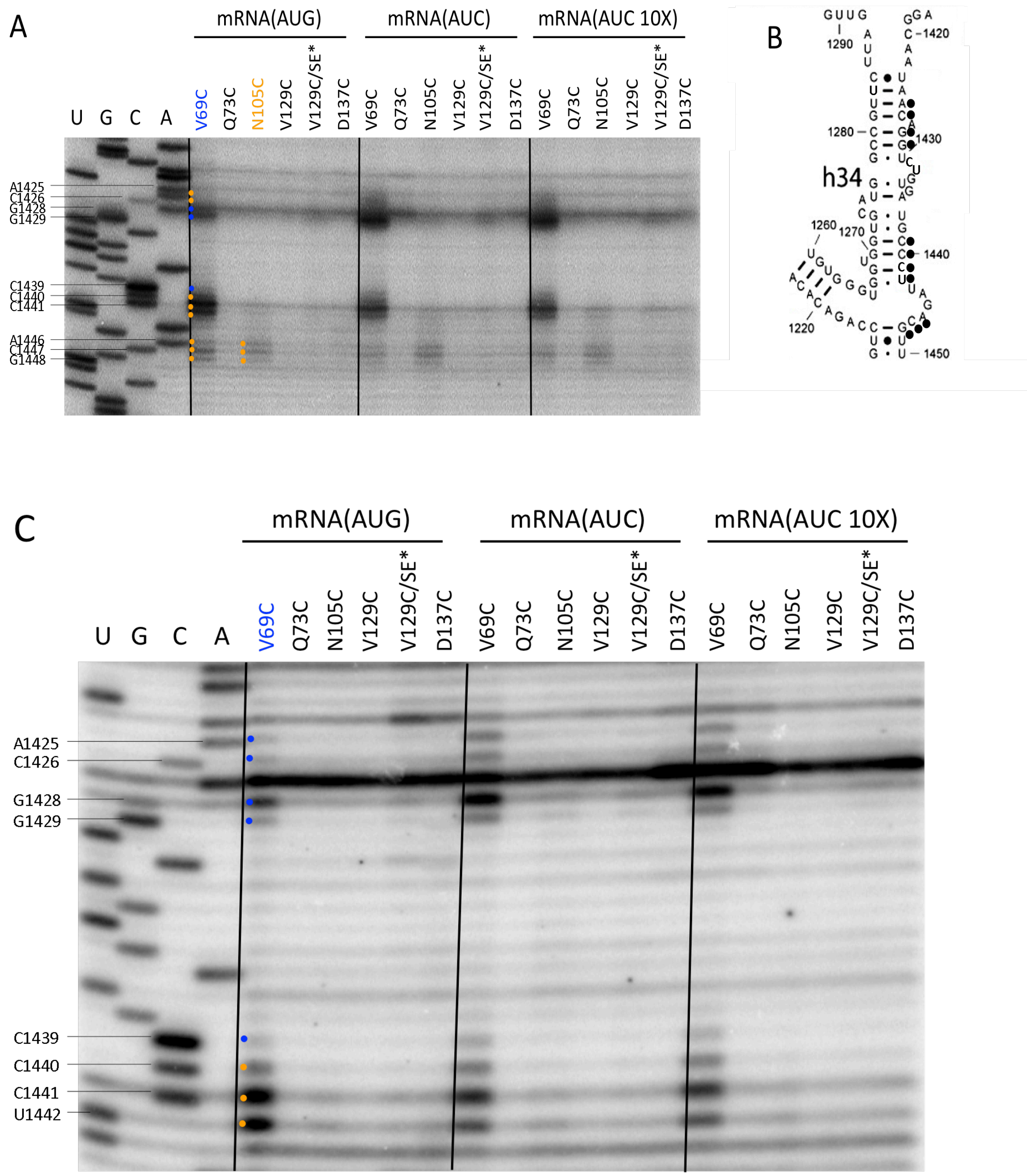

Figure S14. (A-C) Increasing the concentration of mRNA(AUC) by an order of magnitude does not appreciably alter patterns of AUC>AUG cleavage or response to the SE* substitutions in different locations in h34. Experiments were conducted and results presented exactly as described for Figs. S11.

Fig. S15, Zhang et al.

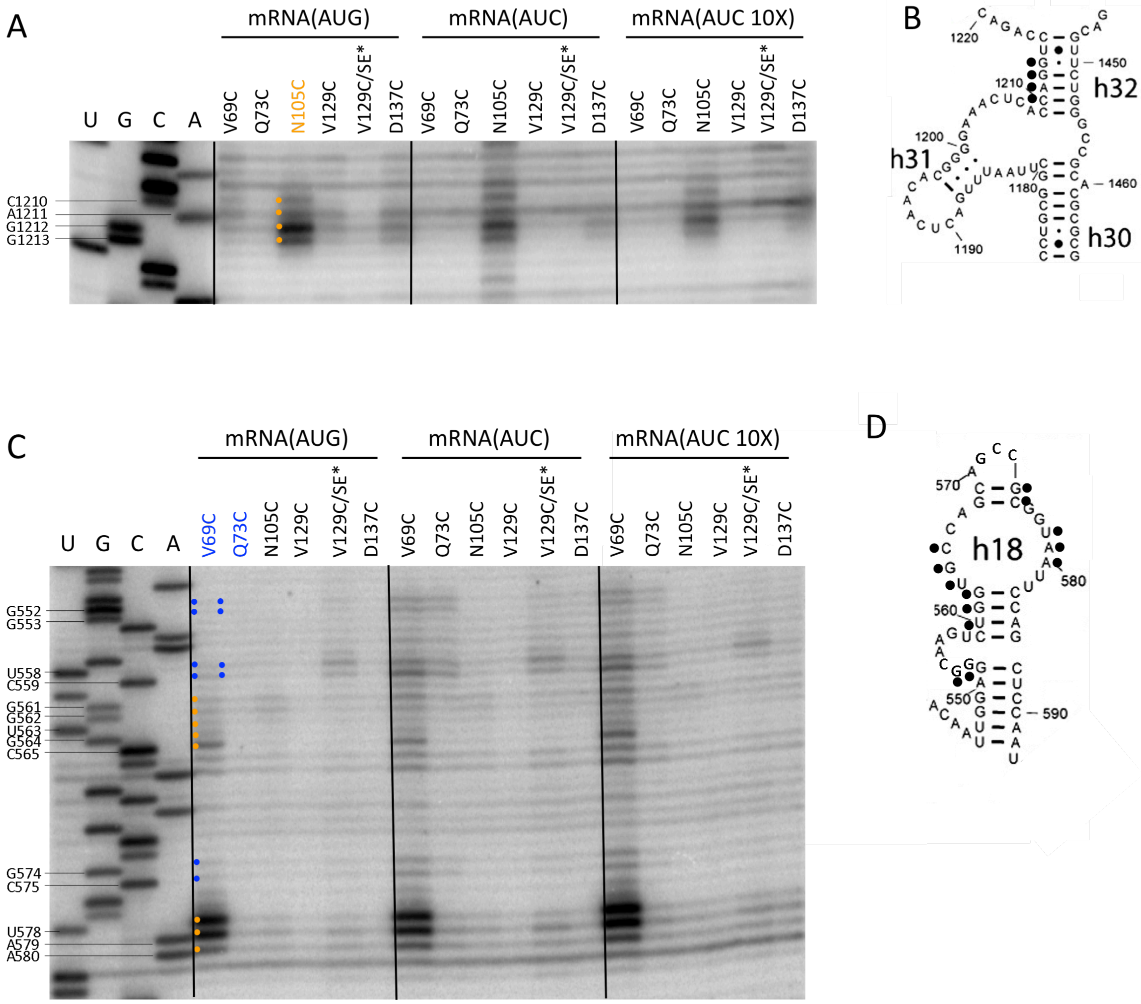

Figure S15. Increasing the concentration of mRNA(AUC) by an order of magnitude does not appreciably alter patterns of AUC>AUG cleavage or response to the SE* substitutions in h32 (A-B) and h18 (C-D). Experiments were conducted and results presented exactly as described for Figs. S11.

Table S1. Summary of directed hydroxyl radical cleavage of 18S rRNA by Fe(II)-BABE derivatives of single-Cys variants of eIF1A[1].

eIF1A derivatives	Constitutive	AUG-suppressed	AUG-enhanced	Altered by SE*
K11C	C1759 U1758 A1635 G1575 C1463 G1462 C1461 U1276 C1274 G1273 G1271 A579 U578	U1761 G1757 A1756 G1638 C1637 C1634 U1578 A1577 A1576 G1429 G1428 C1426 A1425 C575 G574 C559 U558 G553 G552		
K11C/SE*	U1761 C1759 U1758 G1757 A1756 G1638 C1637 A1635 C1634 A1576 G1575 C1463 G1462 C1461 G1429 G1428 C1426 A1425 A579 U578 C575 G574 C559 U558	C559 U558 G553 G552		U1761 G1757 A1756 G1638 C1637 C1634 A1576 G1575 G1429 G1428 C1426 A1425 C575 G574
P22C	C1759 U1758 C1463 G1462 C1461 G1448 C1447 A1446 U1442 C1441 U1276 C1274 G1273 G1271 A580 A579 U578 C565 G564 U563 G562 G561 U560	U1761 G1757 A1756 G1638 C1637 A1635 C1634 U1578 A1577 A1576 G1575 C1440 C1439 G1429 G1428 C1426 A1425 C575 G574 C559 U558 G553 G552		
V69C	C1759 U1758 C1463 G1462 C1461 G1448 C1447 A1446 U1442 C1441 U1276 C1274 G1273 G1271 A580 A579 U578 C565 G564 U563 G562 G561 U560	U1761 G1757 A1756 G1638 C1637 A1635 C1634 U1578 A1577 A1576 G1575 C1440 C1439 G1429 G1428 C1426 A1425 C575 G574 C559 U558 G553 G552		
Q73C	U1758 G1757	U1761 A1756 G1638 C1637 C559 U558 G553 G552	G1760 C1759 C1646 G1645 C1644 U1643 C1463 G1462 C1461	
N105C	G1462 C1461 G1448 C1447 A1446 G1213 G1212 A1211 C1210	C1463		
E124C	G1462 C1461	C1463		
V129C	G1462 C1461	C1463		
V129C/SE*	A1576 G1575 C1463 G1462 C1461			A1576 G1575 C1463
D137C	C1461	C1463 G1462		
G143C	C1461	C1463 G1462		

[1]Constitutive cleavage: equal intensity of cleavage in No-mRNA, mRNA(AUC) and mRNA(AUG) PICs; AUG-suppressed: reduced cleavage in mRNA(AUG) versus No-mRNA and mRNA(AUC) complexes; AUG-enhanced: greater cleavage in mRNA(AUG) versus No-mRNA and mRNA(AUC) complexes; Altered by SE*: reduced or enhanced cleavage by K11C/SE* or V129C/SE* versus K11C and V129C derivatives.